Journal of Biomechanics 47 (2014) 765–772

Contents lists available at ScienceDirect

Journal of Biomechanics

journal homepage: www.elsevier.com/locate/jbiomech
www.JBiomech.com

Effects of mechanical properties and atherosclerotic artery size on biomechanical plaque disruption – Mouse vs. human

Laurent M. Riou [a,1], Alexis Broisat [a,1], Catherine Ghezzi [a], Gérard Finet [b], Gilles Rioufol [b], Ahmed M. Gharib [c], Roderic I. Pettigrew [c,*], Jacques Ohayon [d,e,**]

[a] INSERM, UMR_S 1039, Radiopharmaceutiques Biocliniques, Faculté de Médecine de Grenoble, Grenoble, France
[b] Department of Hemodynamics and Interventional Cardiology, Hospices Civils de Lyon and Claude Bernard University Lyon1, INSERM Unit 886, Lyon, France
[c] Laboratory of Integrative Cardiovascular Imaging Science, National Institute of Diabetes Digestive and Kidney Diseases, National Institutes of Health, Bethesda, MD, USA
[d] Laboratory TIMC-IMAG/DyCTiM, UJF, CNRS UMR 5525, In^{3}S, Grenoble, France
[e] Polytech Annecy-Chambéry, University of Savoie, Le Bourget du Lac, France

ARTICLE INFO

Article history:
Accepted 13 January 2014

Keywords:
Plaque disruption
Mouse
Human
Mechanical properties
Artery size

ABSTRACT

Mouse models of atherosclerosis are extensively being used to study the mechanisms of atherosclerotic plaque development and the results are frequently extrapolated to humans. However, major differences have been described between murine and human atherosclerotic lesions and the determination of similarities and differences between these species has been largely addressed recently. This study takes over and extends previous studies performed by our group and related to the biomechanical characterization of both mouse and human atherosclerotic lesions. Its main objective was to determine the distribution and amplitude of mechanical stresses including peak cap stress (PCS) in aortic vessels from atherosclerotic apoE$^{-/-}$ mice, in order to evaluate whether such biomechanical data would be in accordance with the previously suggested lack of plaque rupture in this model. Successful finite element analysis was performed from the zero-stress configuration of aortic arch sections and mainly indicated (1) the modest role of atherosclerotic lesions in the observed increase in residual parietal stresses in apoE$^{-/-}$ mouse vessels and (2) the low amplitude of murine PCS as compared to humans. Overall, the results from the present study support the hypothesis that murine biomechanical properties and artery size confer less propensity to rupture for mouse lesions in comparison with those of humans.

1. Introduction

Coronary vulnerable plaque rupture and subsequent thrombosis represent the main cause of coronary events, which are responsible for the majority of cardiovascular deaths (Go et al., 2013; Fleg et al., 2012). From a biomechanical point of view, a relationship has been described between the likelihood of plaque rupture and the amplitude of mechanical peak cap stress (PCS) (Richardson et al., 1989; Loree et al., 1992; Cheng et al., 1993; Finet et al., 2004; Ohayon et al., 2008; Speelman et al., 2011; Akyildiz et al., 2011). Accordingly, Richardson et al. (1989) first suggested the potential role of mechanical stress in plaque rupture by demonstrating the influence of the necrotic core on stress concentration in the fibrous cap of atherosclerotic plaques from patients. Loree et al. (1992) characterized the relationship between fibrous cap thinning and the corresponding increase in PCS whereas Cheng et al. (1993) showed that maximal mechanical stress was significantly higher in unstable vs. stable human coronary lesions. More recently, Ohayon et al. (2008) using structural finite element simulations demonstrated that plaque instability is to be viewed not as a consequence of fibrous cap thickness alone but rather as a combination of cap thickness, necrotic core thickness, and arterial remodeling index. Their study provided clues as to why lesions were more prone to rupture at early stages of positive remodeling, which could explain the fast progression and growth of clinically silent plaques.

Mouse models of atherosclerosis are extensively being used to study the mechanisms of atherosclerotic plaque development (Weber et al., 2008) and the results are frequently extrapolated to humans. However, major differences have been described between the widely used apoE$^{-/-}$ mouse model and human atherosclerotic lesions (Bentzon and Falk, 2010) and the determination of similarities and differences between these species has

* Corresponding author.
** Corresponding author at: Laboratory TIMC-IMAG/DyCTiM, UJF, CNRS UMR 5525, In^{3}S, Grenoble, France. Tel.: +33 456 52 0124; fax: +33 456 52 00 22.
E-mail addresses: rpettig@mail.nih.gov (R.I. Pettigrew), jacques.ohayon@imag.fr (J. Ohayon).
[1] Both authors equally contributed.

0021-9290/$ - see front matter © 2014 Elsevier Ltd. All rights reserved.
http://dx.doi.org/10.1016/j.jbiomech.2014.01.020

been extensively addressed recently (Hansson and Heistad, 2007; Schwartz et al., 2007; Jackson et al., 2007; Jackson, 2007; Falk et al., 2007; Rosenfeld and Schwarz, 2007; Rosenfeld et al., 2008; Bond and Jackson, 2011). Specifically, distinct opinions have been expressed regarding the presence and characteristics of murine plaque rupture and the subsequent formation of thrombus. Accordingly, some investigators recommended the replacement of the specific term "rupture" by that of the more general "disruption" when addressing the natural history of mouse atherosclerotic lesion development in comparison with that of humans (Schwartz et al., 2007; Falk et al., 2007). The use of a distinct terminology was motivated by the observation that despite being extremely thin, the cap of murine lesions does not rupture but that plaque disruption is rather generally caused by fissuring of the plaque at the level of lateral xanthomas (Schwartz et al., 2007).

The main objective of the present study was to determine the distribution and amplitude of mechanical stresses including PCS in aortic vessels from atherosclerotic apoE$^{-/-}$ mice, in order to evaluate whether such biomechanical data would be in accordance with the hypothesis of the absence of plaque rupture in mice that was previously suggested by the abovementioned studies. Finite element analysis was used, starting from the zero-stress configuration as obtained using the opening angle technique (Chuong and Fung, 1983; Matsumoto et al., 1995; Rehal et al., 2006; Ohayon et al., 2007), in order to account for residual stresses remaining in the vessel wall in the absence of external load. In addition, differences between murine and human lesions from the point of view of plaque biomechanics will be further discussed, in order to examine whether the mechanical properties of murine plaque constituents, the size of atherosclerotic arteries and the resulting amplitude and distribution of mechanical stresses confirmed or infirmed the hypothesis that murine and human lesions might display differential behaviors with regards to atherosclerotic plaque disruption.

2. Materials and methods

2.1. Experimental protocol

Five weeks-old female apoE$^{-/-}$ mice on a C57/BL6J background ($n=25$) and age-matched wild-type (C57/BL 6J) control mice (n=20) were obtained from Charles River Laboratory. ApoE$^{-/-}$ animals were fed a western-type diet (20% casein milk/0.15% cholesterol – Harlan) whereas control mice remained on chow diet. Control and apoE$^{-/-}$ mice were euthanized by an overdose of pentobarbital at 7, 15, 20, 25 or 30 weeks ($n=3$–5 apoE$^{-/-}$ and control animals/time point). The aorta was harvested and immersed in ice-cold Krebs–Henseleit containing 0.026 mM EDTA (KH). The aortic arch was carefully dissected free from adhesive tissues under a binocular (Discovery V8, Zeiss) and transferred into a mold containing gelatine (25% in KH, 37 °C). The mold was cooled down to 5 °C and the embedded arch was fixed on a sample holder immersed in ice-cold KH. A 200 μm-thick section located between the brachio-cephalic and the left carotid arteries ostia was obtained using a vibratom (HM650V, Microm). The cross-section of the aortic ring was rinsed thrice in KH (37 °C) and cut radially at a site corresponding to the large curvature of the vessel, i.e. in the healthy portion of the aorta localized at the opposite of the small curvature where atherosclerotic lesions reproducibly develop in apoE$^{-/-}$ mice (Fig. 1). The duration of the no-load state from vessel excision to wall vessel incision was reproducible and approximated 60 min. Residual stress/strain (RS/S) dissipation resulted in the opening of the aortic ring. The determination of the opening angle was performed after complete stabilization of the opened vessel (45 min). The aortic arch section immediately adjacent to the 200 μm-thick ring was embedded in paraffin using standard protocols, and 4 μm transversal slices were obtained using a microtom (HM340E, Microm) for histological and immunohistological stainings.

2.2. Histology and immunohistology

Standard trichrome HES staining (Haematoxylin, Erythrosine, Safran) for nuclei, cytoplasm and fibrosis staining as well as Von Gieson staining of elastic lamina, von Kossa staining of calcium carbonate deposits, Vascular Smooth Muscle Cell (VSMC) and macrophage staining were performed on paraffin-embedded sections. VSMC staining was performed using an anti-α-actin antibody (A5691, Sigma) while macrophage staining used an anti-galectin-3 (Mac-2) antibody (CL8942AP, Cedarlane). Briefly, the slices were deparaffinized and rehydrated. Unmasking of tissue antigen was performed for 15 min at 100 °C (Vector Laboratories). Following a 1 h blocking step at room temperature, the primary antibody was applied on the tissue sections, either overnight at 4 °C (anti-galectin-3, 1:10,000) or for 1 h at room temperature (RT) (anti-α-actin, 1:800). The anti-α-actin antibody was directly coupled with the alcalin phosphatase, whereas a 1 h incubation with a biotinylated secondary antibody was needed for galectin-3 staining (1 h at RT). The appropriate chromogen was applied (permanent red or DAB) and the sections were counterstained with haematoxylin.

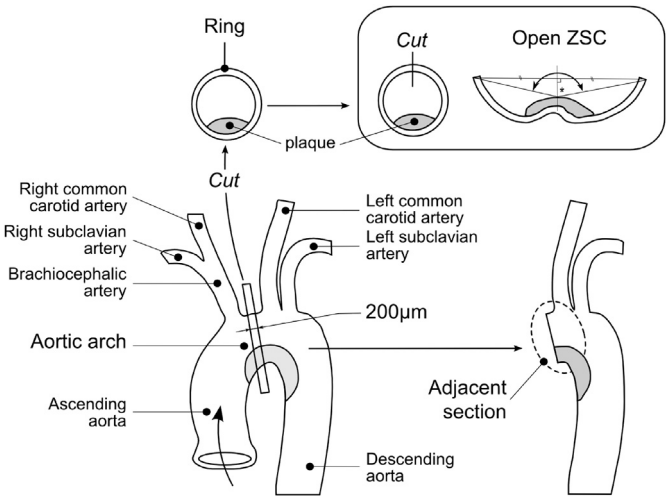

Fig. 1. Schematic view of the mouse aortic arch anatomy. The 200 μm *thick rectangle* indicates the location where aortic rings were sampled along the aortic arch of the apoE$^{-/-}$ mouse. The *gray area* represents an atherosclerotic plaque. Schematic views of typical aortic ring after sampling (closed geometry in the top rectangular frame) and after a radial cut that releases the residual stresses are presented (open geometry in the top rectangular frame). The two extremities of the open ring are used to determine the opening angle α of the aortic ring sample. ZSC: zero-stress geometrical configuration. Adapted from Fig. 1, Ohayon et al. (2012).

2.3. Identification of atherosclerotic lesion constituents

HES, von Gieson, VSMC and macrophage stainings were used to subdivide atherosclerotic lesions into 3 distinct constituents. The cellular fibrosis (CeFb) region was defined as a fibrotic area colonized by VSMC; the hypocellular fibrosis (HyFb) region was defined as a hypocellular area with a robust fibrosis staining on von Gieson and trichrome HES images; the lipid-rich (LpRi) region was defined as the area containing either macrophage-derived foam-cells or vacuoles.

Histological and immunohistological stainings could not be performed directly on the opened sector due to the extreme technical difficulty in obtaining paraffin-embedded opened aortic rings that allowed the preparation of histological slices containing the whole length of the opened vessel. We were therefore forced to use the closed section that was immediately adjacent to that used for open angle determination for histo- and immunohistochemical analysis allowing the determination of wall vessel constituents. Once identified, the sectional vessel geometry was mapped back onto the opened sector using the specific and unique anatomical landmarks that were observed on each lesion, with the process being performed by 2 expert observers.

This identification of atherosclerotic lesion constituents on the opened aortic ring was used for the finite element computation of stress and strain distributions.

2.4. Image analysis and morphometric measurements

The stained atherosclerotic cross-sections were observed using a microscope (Olympus BX41). Digital images were acquired and used for morphometric measurements. From unloaded and closed atherosclerotic cross-sections, neointimal, medial and adventitial thicknesses were measured. These measurements were performed at the level of the small curvature of the aortic arch section where atherosclerotic lesions develop. A planimetric analysis was conducted to determine the area of the lesion and of its constituents. The tortuosity of medial elastic lamina was estimated from von Gieson staining as the arc-to-chord ratio using the formula $\tau = L/C$ with τ: tortuosity, L: length of the elastic lamina, and C: shortest distance between its ends. The stretching index was defined as the inverse of the tortuosity index. The tortuosities of all elastic lamina were calculated for each vessel section and averaged. The opening angle (α) was determined from images of the opened